Fast Association Rates Suggest a Conformational Change in the MHC Class I Molecule H-2D^b upon Peptide Binding

Sebastian Springer,*,† Klaus Döring,‡ Jonathan C. A. Skipper, Alain R. M. Townsend, and Vincenzo Cerundolo

Institute of Molecular Medicine, University of Oxford, Oxford OX3 9DS, U.K.

Received July 17, 1997; Revised Manuscript Received December 18, 1997

ABSTRACT: Major histocompatibility complex (MHC) class I molecules bind peptides in the endoplasmic reticulum (ER). For this binding reaction, when performed in vitro, widely differing association rates have been reported. We have expressed empty soluble H-2D^b class I molecules in Chinese hamster ovary (CHO) cells and generated complete sets of association, dissociation, and equilibrium constants of unmodified peptides using tritium-labeled peptides and stopped-flow fluorescence spectroscopy. We find that (i) the transition midpoint of temperature denaturation (T_m) of the protein is shifted from 30.5 to 56 °C upon the binding of a high-affinity peptide. (ii) With the peptide SV-324-332 (sequence FAPGNYPAL) at 4 °C, the dissociation rate constant of 1.02×10^{-5} s^{-1} and an equilibrium constant of 8.5×10^7 M^{-1} predict an association rate constant of 870 M^{-1} s^{-1} for a simple one-step model of binding. (iii) In contrast, binding of this peptide proceeds much faster, with 1.4×10^6 M^{-1} s^{-1}. These "mismatch kinetics" suggest that peptide binding occurs in several steps, most likely via a conformational rearrangement of the peptide binding groove. The structure of the peptide−class I complex at the time-point of peptide recognition may therefore be different from the equilibrium crystal structures. (iv) Association of modified peptides, in the presence of detergent, or above the T_m of the empty molecule is considerably slower. This might explain why fast on-rates have not been observed in previous studies.

Surveillance of the intracellular protein composition is the basis of the antiviral immune response in mammalian cells. Degradation products of cytosolic proteins, viral or cellular, are transported to the lumen of the endoplasmic reticulum (*1*) and bind there, as peptides of 8−11 amino acids, to MHC[1] class I molecules for subsequent transport to the cell surface and presentation to cytotoxic T lymphocytes (*2*).

The crucial requirement for the surface presentation and in vivo immunogenicity of a peptide is its ability to assemble into a trimeric complex with an MHC class I heavy chain (HC) and β_2 microglobulin (β_2m) and to remain in this complex sufficiently long to reach the cell surface (*3*). The pool of peptides bound to a class I allele displays allele-specific motifs with respect to sequence and length (*4*), and crystal structure analyses of class I molecules with bound peptide have shown that defined class I−peptide interactions occur through these binding motifs, providing the specificity of the binding reaction (*5*).

All natural epitope peptides tested have been found to form stable complexes with the respective class I HC allele and β_2m in vitro (*6*), and no additional factors are necessary for this assembly reaction (*7*). As peptide and β_2m bind cooperatively to the heavy chain (*8*) and, therefore, peptide binding to HC/β_2m complexes occurs at far lower peptide concentrations than peptide binding to free HC (*9*), it is now generally assumed that in the ER, at low peptide concentration, the complex of β_2m and HC forms first, and peptide then binds to this HC/β_2m heterodimer. In vivo, assembly of HC into complexes with peptide and β_2m occurs within 5−20 min of synthesis (*10*), followed by the egress of the formed complexes to the cell surface via the secretory pathway.

To study the binding of peptides to various class I alleles, several in vitro systems have been developed (*3, 7, 11*−*14*). In most of these studies, equilibrium association constants in the range of $K_a = 10^6$−10^8 M^{-1} were determined for the binding of peptides of optimized length and sequence.

In contrast, peptide association rates were found to vary widely between experimental systems. Usually, association was slow, resulting in binding half-times of minutes even at micromolar concentrations of peptides; however, in one study using recombinant soluble molecules, association rate constants of up to 5.9×10^4 M^{-1} s^{-1} were reported for H-2K^b at 23 °C (*7*).

Measurement of association rate constants requires that the class I molecules be free of endogenous peptide so that the dissociation of prebound peptides does not become the

* To whom correspondence should be addressed. C/o Schekman, Department of Molecular and Cell Biology, 401 Barker Hall #3202, University of California, Berkeley, CA 94720-3202. Tel.: (510) 642-6171. Fax: (510) 642-7846. E-mail: springer@uclink4.berkeley.edu.

† Present address: Howard Hughes Medical Institute and Department of Molecular and Cell Biology, University of California, Berkeley, CA 94720-3202.

‡ Max Planck Institute for Biology, D-72076 Tübingen, Germany. Present address: New Chemistry Laboratory, South Parks Road, Oxford OX1 3QT, U.K.

[1] Abbreviations used: CHO cells, chinese hamster ovary cells; D^b, H-2D^b murine MHC class I molecules; ER, endoplasmic reticulum; HC, MHC class I molecule heavy chain; hβ_2m, human β_2 microglobulin; (n)IEF, (native) isoelectric focusing; MHC, major histocompatibility complex; Ni−NTA, nickel nitrilotriacetic acid; R.U., relative units; TAP, transporters in antigen presentation; T_m, transition midpoint of heat denaturation (melting point).

S0006-2960(97)01744-3 CCC: $15.00
Published on Web 02/07/1998

limiting factor. In studies where this was not achieved, the on-rates measured were very low (*15, 16*) and independent of the concentration of added peptide (*17*). In other studies, the peptide was modified by either N-terminal (*18*) or side-chain (*14*) dansylation, by radio-iodination (*7, 19*), or by immobilization onto a sensor surface (*20, 21*). Covalent modification of peptides can significantly alter their kinetic and equilibrium binding properties (*13, 22*), even if the modified residue is not an anchor (see below). Finally, for some of the in vitro assays, class I molecules were isolated from cells via detergent lysis and immunoprecipitation. However, the presence of detergent has been shown to influence the binding behavior of class I (*23, 24*) and the closely related MHC class II molecules (*25*). Also, the binary complexes of class I heavy chains and β_2m are unstable overnight in the presence of detergent (*8*), which makes peptide binding and denaturation competing reactions in these experiments.

We have sought to eliminate these sources of error by establishing a system in which the binding of unmodified peptide to a stable, pure, binary complex of human β_2m and the murine class I heavy chain H-2D^b (D^b) is measured. In the present study, we have used this system to generate full sets of kinetic and equilibrium binding constants. We find that association rates are much faster than previously reported and similar to the rates generally found for the binding of ligands to receptors and antibodies. We therefore find a mismatch between the ratio of kinetic association and dissociation rates and the equilibrium binding constant. This suggests that binding of peptides to class I molecules occurs in more than one kinetic step, possibly involving a conformational transition of the class I molecule in the process.

EXPERIMENTAL PROCEDURES

Expression of Recombinant Soluble D^b and hβ_2m. The cDNA encoding D^b, amplified by the polymerase chain reaction to introduce a hexahistidine tail after amino acid 284 to replace the transmembrane and cytosolic domains, and the cDNA encoding human β_2m were cloned into pEE14 (*26*), each under the control of a separate copy of the human cytomegalovirus promoter−enhancer. The resulting plasmid was introduced into CHO K1 cells as described (*26*). Several rounds of selection in increasing concentrations of L-methionine sulfoximine were performed. Supernatants were tested by an enzyme-linked immunosorbent assay using the 28.14.8S anti-heavy-chain antibody (*27*).

Purification of Recombinant Soluble D^b/hβ_2m Complexes. Protein production was in batch cultures, essentially as described by Bjorkman and collaborators (*28*), with minor modifications. Briefly, transformed CHO cells were grown in GMEM-S medium (First Link, Dudley, U.K.) supplied with 10% dialyzed fetal calf serum (molecular weight cutoff 1000 Da; First Link) and 100 units of penicillin and 100 μg of streptomycin per milliliter (Gibco BRL, Paisley, U.K.), but without addition of glutamine. L-Methionine sulfoximine (Sigma) was added to 160 μM to select for the integrated plasmid. The recombinant heterodimer was isolated from the cell culture supernatant by adsorption to nickel nitrile triacetic acid (Ni−NTA) agarose beads (Qiagen, Crawley, U.K.) in the presence of 10 mM imidazole, either in batch or over a 5 × 20 cm column. Elution was with 100 mM imidazole. The buffer for all subsequent manipulations was phosphate-buffered saline (PBS), pH 7.5. The eluate from the Ni−NTA agarose column was concentrated in Centriprep tubes (Amicon) and applied to a gel filtration column (Sephacryl S-200 HR, 5 × 100 cm, Pharmacia). Two peaks were observed in the elution, the early peak consisting of aggregates of D^b, hβ_2m, and contaminating proteins, the late peak containing mainly D^b/hβ_2m heterodimer as assessed by native gel electrophoresis (data not shown). Fractions corresponding to the late peak were pooled and applied again to a small Ni−NTA agarose column (1 × 10 cm) that was eluted with a gradient of 0−200 mM imidazole in PBS. The purest D^b-containing fractions were dialyzed against 10 mM Tris·Cl pH 7.5, treated with neuraminidase (Sigma; 1 unit per 10 mg protein, 1 h, 37 °C), and applied to a preparative native isoelectric focusing cell (Rotofor, Bio-Rad) in a pH gradient of 6.4−7.0. The D^b/hβ_2m heterodimer focused in two peaks at the acidic end (peptide-occupied or denatured molecules) and in the middle of the gradient, the latter consisting mainly of empty molecules as demonstrated by analytical native isoelectric focusing.

Measurement of Temperature Denaturation. The indicated amount of D^b/hβ_2m heterodimer was heated from 20 to 80 °C in a stirred 1 cm fluorescence cuvette at a rate of 3 min per K. Tryptophan fluorescence (excitation, 295 nm; emission, 345 nm) was recorded on a Perkin-Elmer LS-50B fluorimeter. Temperature readings were taken from the cuvette holder sensor standardized against an in-cuvette thermocouple. The curves were smoothed using the UNIX program xmgr. To obtain the derivative of the temperature curve, differences between consecutive points were calculated.

Peptides. All peptides were synthesized by Neosystems (Strasbourg, France). For all radioligand- and fluorescence-binding assays, only peptide material was used that exhibited a single peak on HPLC. Peptides were dissolved in PBS at 1 mg/mL. Stock solutions were stored in small aliquots at −70 °C or used directly in the case of iodinated peptides. Peptide concentrations were determined by tyrosine absorption measurements.

The SV-324-332 peptide was synthesized by Neosystems and was tritiated by iodination and subsequent reductive tritiation by NEN Du Pont (Boston, MA).

The addition of peptide stock solution to the PBS solution containing the D^b/hβ_2m heterodimer caused no significant shift in pH (data not shown).

Radioligand Binding Assays. A given amount (for equilibrium measurements ca. 5 μg = 100 pmol, for association measurements less as indicated) of D^b/hβ_2m heterodimer was incubated with 10 μL of packed Ni−NTA agarose beads in 500 μL of PBS for 15 min at the indicated temperature. Tritiated peptide was then added and the mixture rotated or stirred. Bound ligand was separated from free by vacuum filtration of the mixture over Wizard minicolumns (Promega) followed by rapid washing with ice-cold PBS containing 0.5% Triton X-100. The detergent wash was necessary to prevent the binding of radiolabeled peptide to the columns; it had no effect on the number of counts bound (data not shown). The D^b molecules on the Ni−NTA agarose beads were eluted with 25 mM EDTA, and radioactivity was determined by scintillation counting. For equilibrium affinity

measurements, the mixture including peptide was allowed to reach equilibrium overnight. (Attainment of equilibrium was confirmed by incubating control samples for longer periods.) Evaluation was by Scatchard analysis or by direct nonlinear least-squares fitting of a binding isotherm to the data (as in Figure 6), taking ligand depletion into account (*29*). For dissociation rate measurements, the mixture was allowed to reach equilibrium overnight and then centrifuged, and the beads were washed four times with PBS. Unlabeled peptide (20 μM) was then added ($t = 0$ for dissociation) and the total volume again brought to 500 μL. Time-points were taken over a range of 48 h; rates were determined by direct nonlinear least-squares fitting to a monoexponential decay curve. For association rate measurements (see Figure 9), filtration was performed at different times shortly after the addition of peptide; rates were determined as for stopped-flow experiments below. Radioligand binding assays from T2D^b cell lysates were performed as in ref *3*.

Fluorescence Spectroscopy. Steady-state fluorescence measurements were done using a Perkin-Elmer LS-50B spectrofluorimeter with a thermostated cuvette holder. Excitation was at 295 nm, emission was monitored at 345 nm. Stopped-flow kinetic measurements were performed on an Applied Photophysics BioSequential DX-17MV apparatus. Relative volumes (10:1) of D^b/hβ_2m heterodimer (final protein cocentration between 20 and 50 nM) and peptide solutions were mixed, and tryptophan fluorescence (excitation at 300 nm) was observed for 1−100 s. Data from 5 to 40 experiments at identical conditions were averaged and fitted to the exponential curve $y(t) = a_1 + a_2t + a_3(1 - \exp(-k_{obs}t))$ using the system's data analysis software. (The linear term a_2t was introduced to compensate for the baseline drift in the spectrophotometric data.) The association constant was derived from a straight-line fit of the k_{obs} values plotted against the peptide concentration, according to the equation $k_{obs} = k_{on}[\text{peptide}] + k_{off}$ (*29*). The residuals shown in Figure 11 (the differences between the data points and the fitted curve) demonstrate that there is no systematic deviation from this equation.

RESULTS

Recombinant Soluble D^b Molecules Are Essentially Peptide-Free. To facilitate purification of the recombinant protein complex, the cDNA encoding the murine MHC class I molecule H-2D^b was modified to replace the transmembrane and cytosolic domains of the protein with a hexahistidine tail that binds specifically to nickel nitrilotriacetic acid (Ni−NTA) agarose. We then expressed this and a cDNA encoding human β_2m (hβ_2m) from one plasmid in CHO cells using the glutamine synthetase-based expression system (*26*) which allows the amplification of integrated plasmid via selection with the glutamine analogue L-methionine sulfoximine (see the Materials and Methods).

From the supernatant of the highest expressing clones, we obtained between 10 and 25 mg of recombinant protein per liter of culture. This was isolated from the cell culture supernatant by Ni−NTA affinity chromatography (*30*), and protein aggregates were removed by Sephacryl S-200 HR gel filtration and a second Ni−NTA column with gradient elution (Figure 1, lanes a−d).

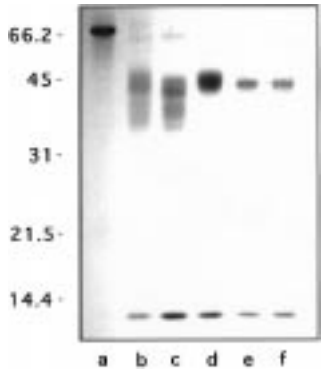

FIGURE 1: Purification of the recombinant soluble H-2D^b/hβ_2m complex. SDS polyacrylamide gel showing the supernatant from CHO cells (lane a), the eluate from the initial Ni−NTA agarose column (lane b), the eluate from the Sephacryl S-200 column (lane c), the eluate pool from the second Ni−NTA agarose column (lane d), the same material after neuraminidase treatment (lane e), and the pool of fractions after nIEF separation (lane f). The positions of molecular weight markers are indicated in the left margin.

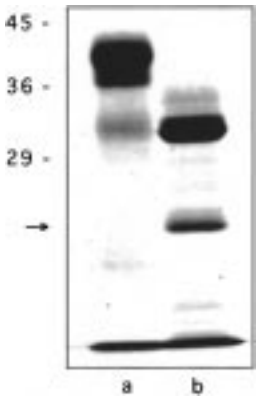

FIGURE 2: Treatment of the purified H-2D^b/hβ_2m complex with *N*-glycosidase F (PNGase). Key: lane a, untreated; lane b, *N*-glycosidase F treated. The positions of molecular weight markers are indicated in the left margin. The arrow indicates the molecular weight of the glycosidase. Glycosylated D^b heavy chain appears as two bands (here overlapping), which probably carry three and two N-linked glycans (there are three potential sites for N-linked glycosylation; compare Figure 3).

Analysis by SDS−PAGE of the purified protein (Figure 1, lane d) shows a sharp band at 12 kDa, corresponding to hβ_2m (11.8 kDa), and a diffuse band corresponding to glycosylated D^b heavy chain. The diffuse band appeared more focused following neuraminidase treatment (Figure 1, lane e) and was converted to a single species of approximately 34 kDa upon *N*-glycosidase F (PNGase, Boehringer) digestion, close to the predicted size of the D^b heavy chain construct of 33.7 kDa (Figure 2). The bands corresponding to D^b heavy chain and hβ_2m could both be precipitated in identical amounts with the monoclonal antibodies 28.14.8S (specific for the α_3 domain) and B22.249 (specific for the folded conformation of the α_1 and α_2 domains) (*8*, *27*, *31*), indicating that these molecules had folded α_1, α_2, and α_3 domains and that hβ_2m was bound to the D^b heavy chain (Figure 3).

Analysis of the protein by mass spectroscopy and isoelectric focusing (IEF) gave no evidence for a heterogeneity in the β_2m population, indicating that no hamster (from the CHO cells) or bovine (from the fetal calf serum) β_2m was detectable in our D^b/hβ_2m preparation (Dennis Benjamin, personal communication).

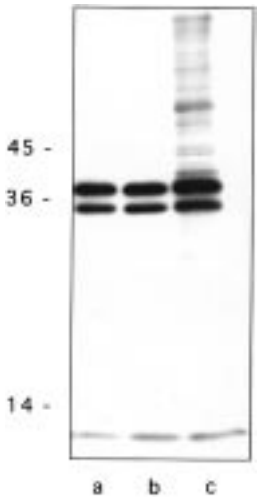

FIGURE 3: Precipitation of [^{35}S]methionine-labeled H-2 D^b/hβ_2m complex from CHO cell supernatant with the monoclonal antibodies 28.14.8S (lane a) and B22.249 (lane b) and with Ni−NTA agarose (lane c) (autoradiograph of an SDS polyacrylamide gel). The positions of molecular weight markers are indicated in the left margin. Equivalent amounts of D^b heavy chain and hβ_2m are precipitated with 28.14.8S and B22.249, indicating that the large majority of D^b heavy chains are associated with hβ_2m and folded correctly. The weaker band below the main heavy chain band probably arises from a missing N-linked glycan (compare Figure 2).

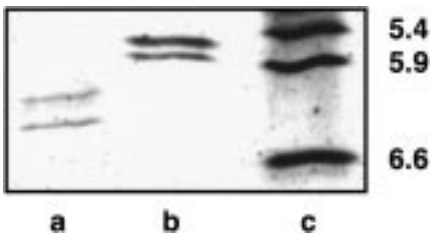

FIGURE 4: Native isoelectric focusing gel of the purified H-2D^b/hβ_2m complex before (lane a) and after (lane b) addition of 20 μM NP$_{68}$-Y367-374 peptide. The isoelectric points (IEPs) of the markers in lane c are indicated on the right margin. The doublet structure of the bands is possibly due to incomplete neuraminidase digestion, although on SDS−PAGE a single band is observed (Figure 1). Both bands exhibit an IEP shift upon exposure to peptide.

On native IEF (nIEF) gels, the material purified by gel filtration separated into two groups of bands, one of which was displaced when a charged peptide was added to the sample prior to focusing. These "peptide-responsive" bands, presumably corresponding to empty D^b/hβ_2m complexes, were purified by preparative nIEF in solution on a pH 6.4 to 7.0 gradient. The protein peak in the more basic fractions contained D^b/hβ_2m complex which shifted entirely on nIEF gels upon addition of charged peptide, indicating that at least the great majority of it was now able to bind exogenously added peptide (Figure 4).

To further examine whether our preparation of D^b/hβ_2m was able to bind peptide, we recorded thermal denaturation curves following the tryptophan fluorescence of the protein (Figure 5). The IEF-purified protein showed a sharp and uniform transition with a midpoint (T_m) at 30.5 °C. This T_m shifted to 56 °C when optimal-binding NP$_{68}$-Y367-374 (sequence YSNENMDAM) peptide was present in excess, suggesting that the protein could be stabilized by peptide binding. With NP$_{68}$-Y367-379 (sequence YSNENMDAMESSTL), a T_m of 41 °C was observed, indicating a

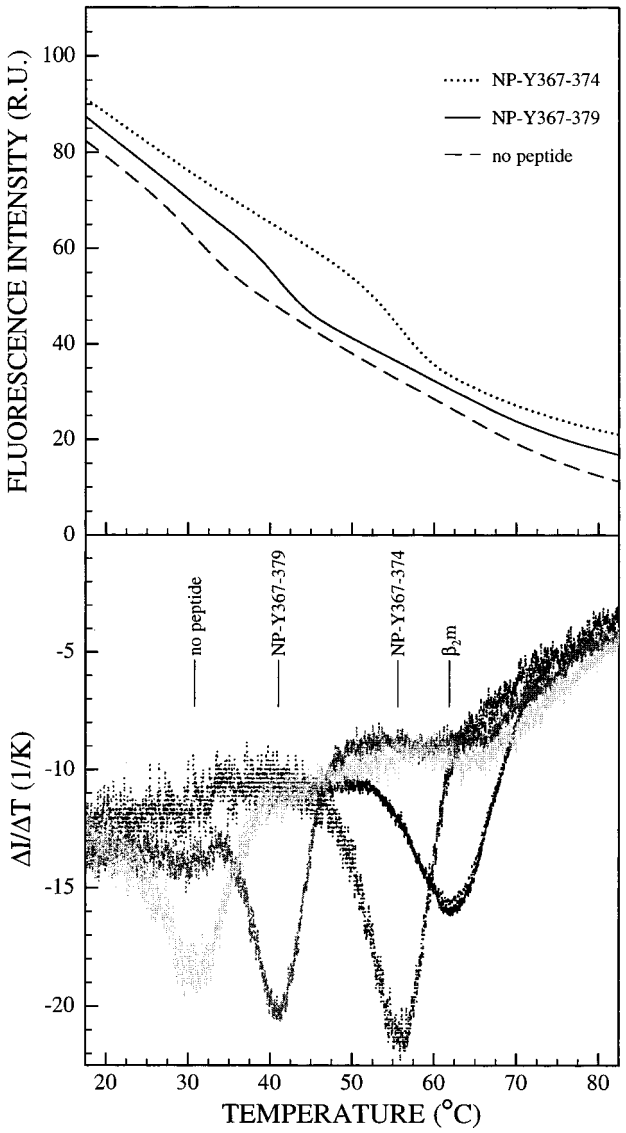

FIGURE 5: Thermal denaturation of the H-2 D^b/hβ_2m complex. Tryptophan fluorescence (upper panel) and first derivative of tryptophan fluorescence (lower panel; see materials and methods) of 50 nM H-2D^b/hβ_2m complex without peptide (no peptide) and with saturating amounts (1 μM) of NP$_{68}$-Y367-374 and NP$_{68}$-Y367-379, or of β_2m alone (β_2m). R.U. = relative units.

lower stabilization energy and therefore a lower binding constant as a result of the C-terminal elongation of this peptide. The complex with the SV-324-332 peptide had an intermediate T_m of 50 °C (data not shown). The T_m of hβ_2m alone was determined as 62 °C in this assay, indicating that the denaturation signals at lower temperatures originated from the D^b heavy chain.

In earlier work, it was shown that complexes of D^b heavy chain with murine (*8*) or human β_2m (Vincenzo Cerundolo, unpublished) dissociate during overnight incubation in detergent cell lysates at 4 °C. In contrast to these observations, our purified D^b/hβ_2m complex was stable in phosphate-buffered saline (PBS) at 4 °C for at least 10 days without change in its peptide-binding properties (data not shown). The instability of the binary complex in cell lysates may be due to a denaturing effect of the detergent, similar to the slowing effect of detergent on peptide association (see below). Destabilization of HC/β_2m complexes in vitro has also been found for H-2K^b (*7*) and H-2K^d (*13*).

Table 1: Determined and Predicted Binding Constants for Peptides to H-2D^b/hβ_2m[a]

peptide	T (°C)	K_a ($\times 10^6$ M^{-1}) ± SEM, $n = 3$	$k_{off} \pm$ SD ($\times 10^{-6}$ s^{-1})	k_{on} ($\times 10^3$ M^{-1} s^{-1}) predicted	$k_{on} \pm$ SD ($\times 10^3$ M^{-1} s^{-1}) measured
recombinant protein					
SV-324-332	16.5	46 ± 5.7	40.5 ± 0.5	1.86	1900 ± 180
	4	85 ± 5.9	10.2 ± 0.2	0.87	1360 ± 180
NP_{68}-Y367-374	37				0.28 ± 0.06
	16.5				1790 ± 130
	4				612 ± 3
NP_{68}-Y367-374G9	16.5				687 ± 7
NP_{68}-Y367-379	16.5				340 ± 25
T2D^b cell lysate					
SV-324-332	4	84 ($n = 1$)	3.3	0.28	35.6
SV-324-332[†]	4	20 ± 6.1	3.15	0.063	8.6

[a] Dissociation rate constants (k_{off}) measured by dissociation of tritiated peptide in the presence of unlabeled competitor; equilibrium constants (K_a) measured by radioligand binding assay using trititated peptide. Association rate constants (k_{on}) with recombinant H-2D^b/hβ_2m measured by stopped-flow fluorescence spectroscopy. In the T2D^b cell lysate, association rate constants measured by radioligand binding assay (see Materials and Methods). [†] Data for iodinated peptide. Errors on the constants from cell lysate binding assays are estimated to 20%; elsewhere they are the standard deviation of the curve fits (SD) or the standard error of the mean of multiple determinations (SEM, with the number of determinations given as n). Predicted $k_{on} = K_a\ k_{off}$. Sequences of peptides (single letter code): SV-324-332, FAPGNYPAL; NP_{68}-Y367-374, YSNENMDAM; NP_{68}-Y367-374G9, YSNENMDAG; NP_{68}-Y367-379, YSNENMDAMESSTL.

To examine whether the D^b/hβ_2m complex was forming higher-order oligomers, we performed analytical ultracentrifugation of the neuraminidase-treated pure protein. We obtained a molecular weight of 46820 ± 460 Da for the empty D^b/hβ_2m molecule and 47790 ± 1000 Da for the complex with NP_{68}-366-374 peptide bound. These values are slightly above the molecular weights of 45 511 and 46 493 Da predicted for the unglycosylated complexes, the difference probably being due to some remaining glycosylation of the D^b heavy chain. The comparable values before and after peptide binding indicate that D^b was present in the heterodimeric complex of heavy chain and hβ_2m but not in larger aggregates and that it remained so after the binding of peptide.

We determined the extinction coefficient at 280 nm of the D^b/hβ_2m complex as $\epsilon = 100\,000 \pm 5000$ M^{-1} cm^{-1} based on calculations (*32*) and protein concentration determinations in comparison to bovine serum albumin.

Determination of Equilibrium Affinity Constants. Equilibrium binding of tritiated Sendai virus peptide SV-324-332 (sequence FAPGN[^{3}H]-YPAL) (*33*) to recombinant D^b was saturable with association constants of $K_a = 4.6 \times 10^7$ M^{-1} at 16.5 °C and 8.5×10^7 M^{-1} at 4 °C (Figure 6, and Table 1). These numbers agree with affinity constants of class I molecules for optimal-length peptides determined by us and others (*3*, *7*, *13*).

Interestingly, it is visible from Figure 6 that the maximum concentration of binding sites as determined by the radioligand assay only reached 70−80% of the added protein as determined by absorption spectroscopy. We reasoned that this could be explained if the D^b/hβ_2m complex was partially dissociated and the free D^b heavy chain unable to bind peptide under the conditions of the assay. Free D^b heavy chain has a far lower affinity for peptide than the D^b/hβ_2m complex (*9*).

We therefore investigated whether there were detectable amounts of free D^b heavy chain present in our preparation. In a thermal denaturation experiment in the absence of peptide, we saw no effect on the T_m at 30.5 °C when 100 nM exogenous hβ_2m was added in excess (Figure 7). At 2 μM excess hβ_2m, there was a small shift of the T_m to 33 °C

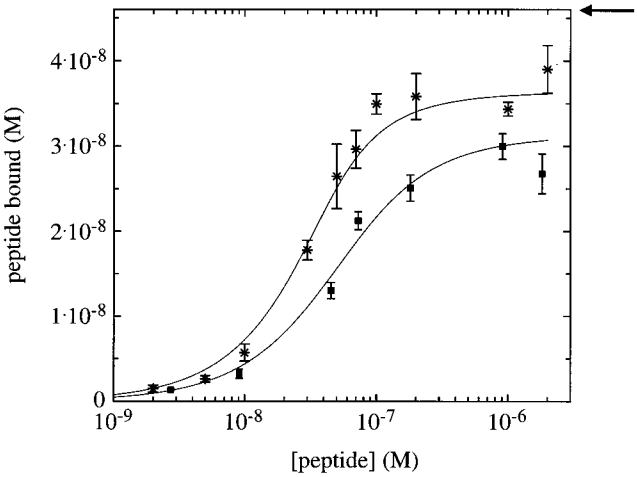

FIGURE 6: Binding of tritiated SV-324-332 peptide (FAPGNYPAL) to recombinant soluble H-2 D^b/hβ_2m complexes at 16.5 °C (asterisks) and at 4 °C (squares). Data are the means of triplicates. The curves are binding isotherms calculated for the affinity constants shown in Table 1. The arrow marks the amount of D^b that was added to the reaction (4.6 nM) as measured by absorption at 280 nm.

that we ascribe to the stabilization of already existing D^b/hβ_2m complexes by the high external concentration of one subunit. Under all three conditions tested, the shape of the transition minimum in the first derivative is very similar, indicating that no change in the nature of the transition and no multiple transitions are occurring. Also, in the melting experiments in the presence of peptide (Figure 5), there is only one melting transition detectable in the presence of peptide, indicating that no substantial amounts of unreacted free heavy chain were present in the assay.

Another possibility is the presence of some denatured D^b heavy chain; however, in the ultracentrifugation and upon incubation at 4 °C over several weeks, no larger protein aggregates were detectable in our preparation. We therefore concluded that the missing 20−30% protein in the equilibrium binding assay could most likely be explained either by an imprecise estimate of the molar extinction coefficient of the protein, which would lead to an error in the determination of the protein concentration by absorption spectroscopy, or

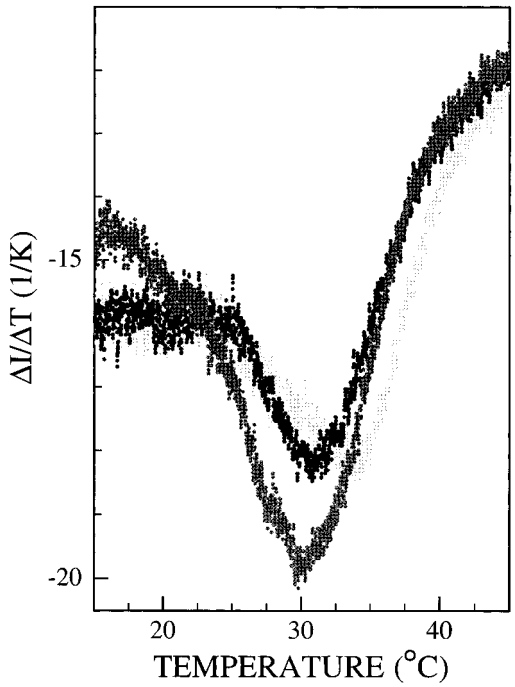

FIGURE 7: Effect of additional hβ_2m on the thermostability of the H-2D^b/hβ_2m complex. Thermal denaturation experiment with 270 nM H-2D^b/hβ_2m in the presence of no (gray), 100 nM (black), and 2 μM (light gray) additional hβ_2m. The first derivative of the thermal denaturation curve is shown. A stabilization shift is observed with 2 μM additional hβ_2m.

by the assumption that some of the protein was already occupied by high-affinity peptides and therefore failed to bind exogenous peptide in the equilibrium assay.

Determination of Dissociation Constants. We then examined the dissociation of tritiated optimal-length SV-324-332 peptide from the D^b molecules in the presence of a large excess of unlabeled peptide (Figure 8). To avoid any complicating effects of dissociation of hβ_2m from the complex, 1 μM additional hβ_2m was included in all measurements. Dissociation obeyed first-order kinetics with half-times of 5.5 h at 16.5 °C and 27 h at 4 °C (dissociation rate constants $k_{off} = 4.1 \times 10^{-5}$ s^{-1} and 1.0×10^{-5} s^{-1}, respectively) in agreement with the slow dissociation rates of peptides from class I molecules found previously (*3, 7, 11, 21*).

Prediction of an Association Rate Constant. The measurements of the equilibrium association and dissociation rate constants allow the prediction of an association rate constant. If the binding of peptides to H-2D^b follows a single-step mechanism

$$D^b + \text{peptide} \underset{k_{off}}{\overset{k_{on}}{\rightleftharpoons}} (D^b \cdot \text{peptide})$$

the law of mass action equates the equilibrium affinity constant K_a to the ratio of the kinetic association and dissociation rate constants (k_{on}/k_{off}). Under this assumption, the association rate constant can be predicted from the above values for K_a and k_{off} as $k_{on} = 1860$ M^{-1} s^{-1} at 16.5 °C and 870 M^{-1} s^{-1} at 4 °C (Table 1) or association half-times of approximately 1.0 and 2.2 h at 100 nM peptide concentration.

We therefore used a radioligand-binding technique (*19*) to determine the association rate of tritiated SV-324-332 peptide with the D^b/hβ_2m complex (Figure 9). Surprisingly, the value obtained at 4 °C (4.4×10^5 M^{-1} s^{-1}) was almost 2 orders of magnitude greater than predicted. This was too fast to be accurately measured in a radioligand assay; therefore, a different technique was necessary.

Peptide Binding to D^b Enhances Tryptophan Fluorescence. We had observed that the natural tryptophan fluorescence (excitation at 295 nm) of the recombinant D^b/hβ_2m dimer was altered upon the binding of peptide in a sequence-specific manner: when saturating concentrations (100 nM) of SV-324-332, NP$_{68}$-366-374, or NP$_{68}$-Y367-374 (sequence YSNENMDAM) peptides were added to the D^b/hβ_2m complex, fluorescence emission at the maximum increased by up to 22% (Figure 10). This was accompanied by a shift of the emission maximum toward shorter wavelengths (blue shift) by 2 nm. Upon addition of a nonspecific peptide, NP$_{68}$-91-99 (KTGGPIYKR), no increase was seen; the peptides alone, containing no tryptophans, gave no signal.

An increase of tryptophan fluorescence and a blue shift of the emission maximum upon ligand binding indicate that the emitting tryptophan indole groups are sensing an environment of lower dielectric constant, that is, higher hydrophobicity (*34*). In the crystal structure of D^b with the NP$_{68}$-366-374 peptide, three tryptophan side chains interact directly with the peptide: residue 167 contacts the N terminus, while 147 and 73 form a hydrophobic ridge over which a C-terminal bulge in the peptide forms (*35*). To determine whether the fluorescence effect upon peptide binding was caused by a direct interaction of the peptide with tryptophans in the binding groove or by some secondary effect of peptide binding (such as a conformational alteration of the protein), we tested the peptide LCMV GP-92-101 (sequence CSANNSHHYI) (*36*) in the fluorescence assay. We hypothesized that in the binding of the peptides NP$_{68}$-366-374 (ASNENMDAM; amino acids predicted to contact one of the D^b tryptophans are underlined), NP68-Y367-374 (YSNENMDAM), and SV-324-332 (FAPGNYPAL), hydrophobic amino acid side chains from the peptide contact one or several of the tryptophans in the binding groove, and cause the fluorescence increases. In contrast, in the CSANNSHHYI peptide, among the potential contact residues are one cystein and two histidines. These amino acids are strong quenchers of tryptophan fluorescence (*37*). If the change in fluorescence upon peptide binding was due entirely to a conformational alteration of the D^b/hβ_2m complex, no difference in the signal should be observed between the CSANNSHHYI peptide and the three others. If, on the other hand, the fluorescence signal originated from the direct interaction of the peptide with the D^b/hβ_2m complex, a quenching effect and not an increase of the fluorescence would be expected with the CSANNSHHYI peptide. Indeed, a fluorescence decrease of 4.5% was found upon binding of CSANNSHHYI at saturating concentrations (Figure 10), indicating that direction and magnitude of the fluorescence effect are dependent on the sequence of the peptide.

We therefore conclude that the fluorescence alteration originates from interactions between the peptide and tryptophan side chains of the D^b molecule that are the result of direct and sequence-specific binding of the peptide. Natural tryptophan fluorescence spectroscopy thus provides a novel method for following the association of peptides to H-2D^b in solution in real time. It avoids errors from the modifica-

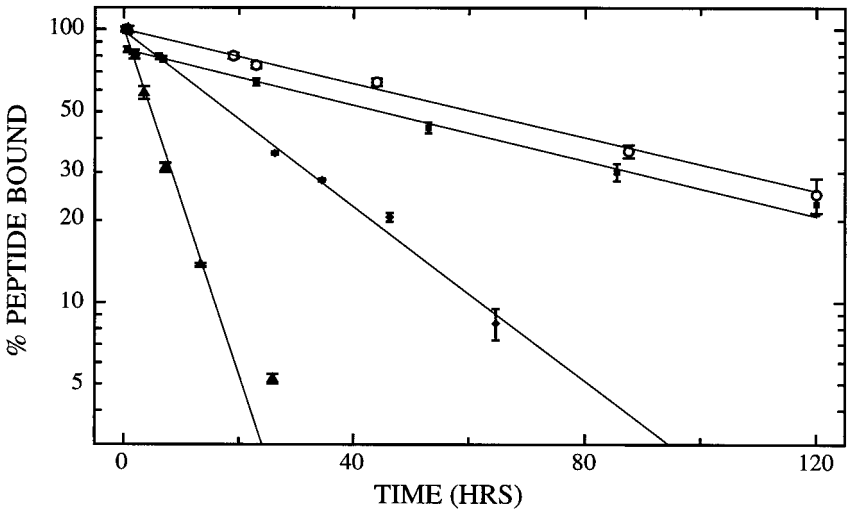

FIGURE 8: Dissociation rates of the SV-324-332 peptide (FAPGNYPAL) from H-2D^b/hβ_2m complex (averages of three experiments). Triangles, recombinant protein and tritiated peptide, 20 °C; diamonds, recombinant protein and tritiated peptide, 4 °C; circles, recombinant protein and iodinated peptide, 4 °C; squares, T2D^b cell lysate and tritiated peptide, 4 °C. The straight lines represent nonlinear least-squares fits of exponential functions (parameters in Table 1). Only in the experiment from cell lysate, an initial rapid drop of the bound radioactivity is seen as described earlier (*3*); the time-point for $t = 0$ was therefore omitted from this curve fit.

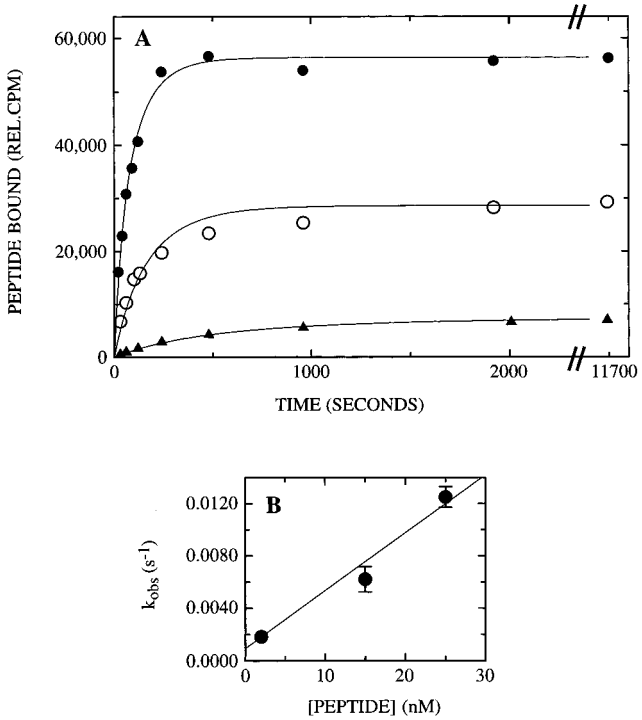

FIGURE 9: Association rate of tritiated SV-324-332 peptide to the recombinant H-2D^b/hβ_2m complex measured by the radioligand assay. Panel A, binding curves: 25 nM peptide, 24.5 nM D^b (closed circles); 15 nM peptide, 4.9 nM D^b (open circles); 2 nM peptide, 4.5 nM D^b (triangles). The lines represent simple exponential curve fits. Panel B: apparent on-rates (k_{obs}) from panel A, plotted against peptide concentration. The line represents a least-squares fit with a slope (association rate constant) of $(4.4 \pm 0.33) \times 10^5$ M^{-1} s^{-1}. One more data point between 2000 and 11 700 s is not shown but used in the fits.

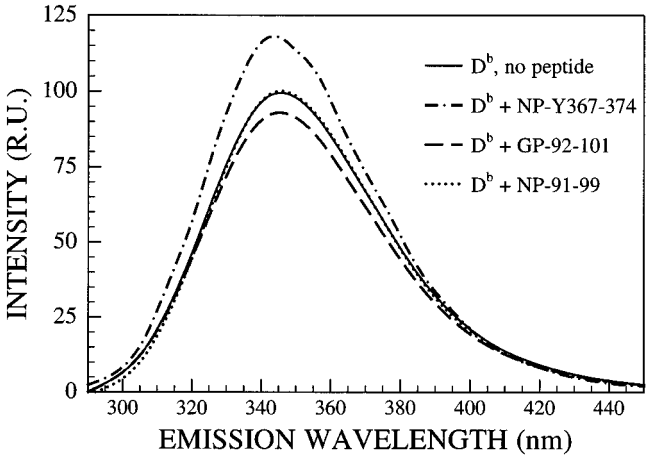

FIGURE 10: Sequence-specific alteration of the tryptophan fluorescence of the soluble H-2 D^b/hβ_2m complexes upon peptide binding. Fluorescence emission scans, excitation at 280 nm. The curves are normalized to the emission maximum of the empty complex = 100 R.U. (relative units). Solid line: 100 nM D^b/hβ_2m, no peptide added (λ_{max}(wavelength of emission maximum) 345.5 nm). Dashed and dotted line: 100 nM D^b/hβ_2m, 100 nM NP$_{68}$-Y367-374 peptide (λ_{max} = 343.5 nm). Dotted line: 100 nM D^b/hβ_2m, 20 μM NP-91-99 peptide (λ_{max} = 345.5 nm). Dashed line: 100 nM D^b/hβ_2m, 100 nM GP-92-101 peptide (λ_{max} = 345.3 nm). The peptides by themselves exhibit no fluorescence (data not shown).

tion of either partner by radio-iodination, fluorescent labeling, or immobilization on sensor surfaces.

Fast Peptide Binding Measured by Stopped-Flow Fluorescence. We then used tryptophan fluorescence emission in a stopped-flow method (*38*) to measure the association of peptides with the soluble D^b/hβ_2m complex over a range of peptide concentrations from 100 nM to 20 μM (Figures 11 and 12; values summarized in Table 1). Plots of the observed association rate against the concentration of peptide were linear and nonsaturable in the range tested, indicating that we were observing a second-order reaction. From the slope of the least-squares fits to the data (see materials and methods), the association rate constant of the SV-324-332 peptide was determined as 1.4×10^6 M^{-1} s^{-1} at 4 °C; the value for NP$_{68}$-Y367-374 was 6.1×10^5 M^{-1} s^{-1} at 4 °C. Values at 16.5 °C were somewhat increased, 1.9×10^6 M^{-1} s^{-1} for SV-324-332, and 1.8×10^6 M^{-1} s^{-1} for NP$_{68}$-Y367-374.

To assess the potentially complicating effects of hβ_2m association and dissociation, we also measured the binding of SV-324-332 at 16.5 °C in the presence of 100 nM

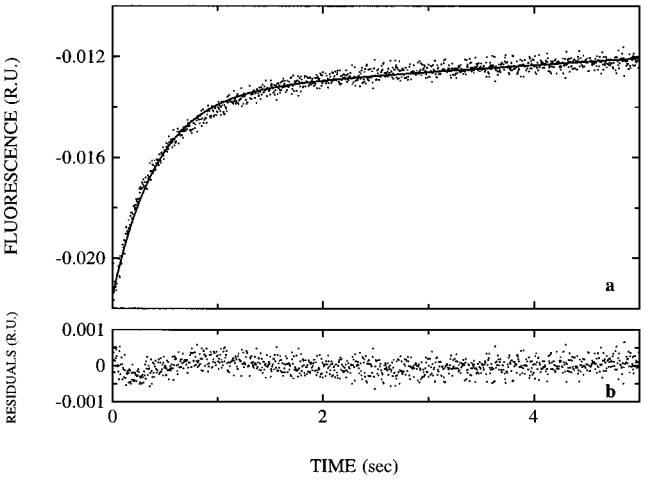

FIGURE 11: Binding of 1 μM NP-Y367-374 peptide to 100 nM H-2D^b/hβ_2m measured by stopped-flow fluorescence spectroscopy (panel a; RU = relative units). Data are the mean of 35 independent measurements. The nonlinear least-squares fit of the binding function (see Materials and Methods; panel b, residuals of the curve fit) gives $k_{obs} = 2.38 \pm 0.022$ s^{-1}. The standard errors of the mean were in the range of 10−15% of the means.

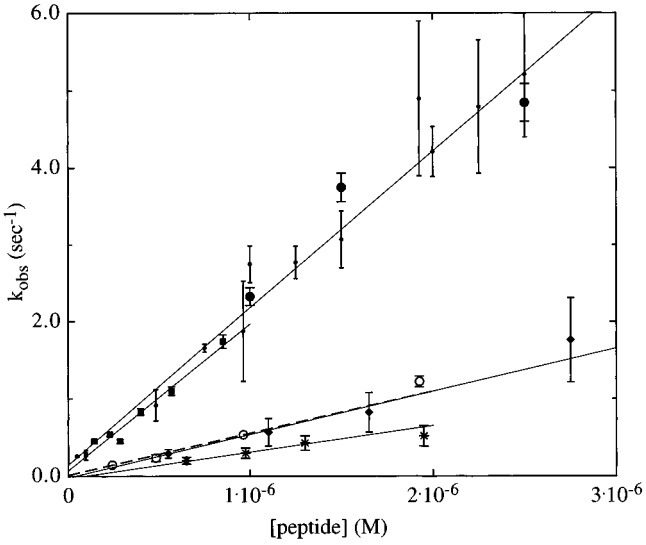

FIGURE 12: Fluorescence stopped-flow association rates of peptides to soluble H-2D^b/hβ_2m complex. Small filled circles and continuous line, NP$_{68}$-Y367-374, 16.5 °C; large filled circles, NP$_{68}$-Y367-374, 16.5 °C plus additional 100 nM hβ_2m; squares, SV-324-332, 16.5 °C; open circles and short dashed line, NP$_{68}$-Y367-374, 4 °C; diamonds, NP$_{68}$-Y367-374G9, 16.5 °C; asterisks, NP$_{68}$-Y367-379, 16.5 °C. The slope of the straight-line fit gives the association rate constant. Association rate constants are listed in Table 1. For NP$_{68}$-Y367-379 and NP$_{68}$-Y367-374G9, not all data points used to derive the curve fits are in the range shown.

additional hβ_2m. In this experiment, no difference was seen in the association rates obtained without additional hβ_2m (Figure 12). We therefore concluded that association between potential free D^b heavy chain and hβ_2m was either not taking place or too slow to be detected in the stopped-flow assay.

Alterations to the optimum peptide sequence reduced the association rate constant. When the C-terminal anchor residue of the NP$_{68}$-Y367-374 peptide, methionine, was replaced by a glycine, the association rate constant dropped to 687 × 10^3 M^{-1} s^{-1} at 16.5 °C; when the peptide was extended by five amino acids to give NP$_{68}$-Y367-379, a rate of 340 × 10^3 M^{-1} s^{-1} was observed.

Influence of Thermal Denaturation on Peptide Binding. We reasoned that the fast association of peptides with class I molecules might not have been reported in previous studies because either modification of peptides was influencing the binding kinetics, detergent was present, or the binding was examined at temperatures above the melting point of the empty molecule (*15*). We therefore tested peptide binding under some of these conditions (Table 1).

The association rate of the peptide, NP$_{68}$-Y367-374, increased from 6.1 × 10^5 M^{-1} s^{-1} at 4 °C to 1.8 × 10^6 M^{-1} s^{-1} at 16.5 °C. However, if the temperature was raised further to 37 °C, above the transition midpoint (T_m) of thermal denaturation as measured by tryptophan fluorescence (30.5 °C; see above), the association rate dropped sharply to 275 M^{-1} s^{-1}, i.e., by nearly 4 orders of magnitude. (This value, too low to be measured by stopped-flow technology, was determined by fluorescence enhancement in a steady-state experiment in a conventional fluorimeter, using a stirred cuvette.) This suggests that, upon melting, the binding site had undergone a denaturation process that was only slowly reversible by the binding of peptide. Upon cooling of the empty protein back to 4 °C, we again observed fast binding kinetics (data not shown), demonstrating that the 30.5 °C thermal denaturation of the molecule was reversible.

Influence of Detergent and Peptide Modification. As we had noticed that the presence of detergent cell lysate had a denaturing effect on the peptide-free D^b/hβ_2m complex (see above), we next sought to determine whether the presence of detergent, cell lysate, or covalent modification of the peptide by iodine had any effect upon the binding kinetics. We therefore measured the binding parameters of tritiated and iodinated SV-324-332 peptide to cellular wild-type D^b molecules in detergent lysates of T2D^b cells at 4 °C using methods described previously (*3*) and found equilibrium and dissociation constants similar to those measured with recombinant molecules (Table 1). In contrast, the association rate constant of tritiated peptide was reduced from 1.4 × 10^6 M^{-1} s^{-1} to 3.6 × 10^4 M^{-1} s^{-1} in the presence of detergent cell lysate. A similar value was obtained when recombinant protein was used in the presence of detergent (data not shown). With SV-324-332 peptide iodinated on the tyrosyl side chain (position 6), the association constant was reduced further to 8.6 × 10^3 M^{-1} s^{-1}. We therefore conclude that the presence of detergent, cell lysate, and the iodination of peptide, even at nonanchor residues, all slow the binding of peptides to D^b. This might explain why other researchers, using cell lysates or modified molecules, have always found lower association rate constants.

Stability of the Initial D^b−Peptide Complex. Finally, we investigated whether an unstable intermediate was present in the D^b−peptide binding reaction (Figure 13). We therefore attempted to displace the SV-324-332 peptide which gives a small fluorescence enhancement (3% at saturation), at different times after binding to D^b, with an excess of NP$_{68}$-Y367-374 peptide which gives a higher signal (16%). As judged by its ability to increase the T_m of the protein, NP$_{68}$-Y367-374 (56 °C) and SV-324-332 (50 °C) have comparably high affinities for D^b/hβ_2m. Because the association rate constant of NP$_{68}$-Y367-374 is very high, the resulting fluorescence increase is controlled by the dissociation of the prebound peptide.

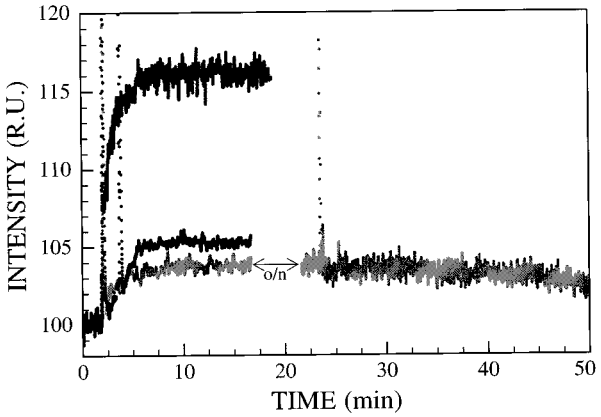

FIGURE 13: Peptide-exchange experiment to determine the stability of newly formed D^b-peptide complexes by steady-state tryptophan fluorescence. 100 nM D^b/hβ_2m complex, 100 nM excess hβ_2m. Gray (upper) curve: control experiment. Addition of NP$_{68}$-Y367-374 peptide to 5 μM (at 2 min). Black (middle) curve: exchange shortly after binding. Addition of SV-324-332 peptide to 500 nM (at 2 min), then 100 s later addition of NP$_{68}$-Y367-374 peptide to 5 μM to attempt displacement. Light gray (lower) curve: exchange from equilibrium. Addition of SV-324-332 peptide to 500 nM (at 2 min), then incubation for 16 min. Further incubation overnight to reach equilibrium (o/n in the figure), then addition of NP$_{68}$-Y367-374 peptide to 5 μM (at 23 min in the figure) to attempt displacement. The slow decrease of this trace is due to photobleaching of the sample.

At 20 °C, 500 nM SV-324-332 peptide were added to 100 nM D^b/hβ_2m, and the fluorescence increase was followed. After an overnight incubation, an excess of NP$_{68}$-Y367-374 peptide (5 μM final concentration) was added in an attempt to displace the SV-324-332 peptide from the initial complex. No increase in the fluorescence, and therefore no displacement of peptide, was observed in the duration of the recording (30 min after the addition of the second peptide) or in an emission spectrum recorded 2 h after the continuous recording.

We then performed the same experiment very shortly after the first addition of peptide. One hundred seconds after the SV-324-332 peptide, NP$_{68}$-Y367-374 was added to 5 μM (final concentration). However, there was only a small increase in the fluorescence, which we believe is due to the binding of excess peptide to previously unreacted D^b/hβ_2m. Therefore, we find no evidence that an unstable intermediate exists at an early stage of the binding reaction.

DISCUSSION

In this study, we have used a stable preformed complex of a MHC class I heavy chain with β_2m to examine the binding of peptide to the complex in a pure system. We decided to use the complex of H-2D^b heavy chain with human β_2m because this combination is more stable in vitro than the complex with murine β_2m, yet exhibits identical antigen presentation characteristics in vivo (*3*). The purification procedure avoids denaturation and renaturation steps, attempting to keep the protein native and active at all times; moreover, the protein is never exposed to detergent, which has a denaturing effect on the complex and slows down binding kinetics (see the previous text). Although peptide-occupied complexes, initially present to about 50% of the protein as determined by nIEF, are largely removed (Figure 4), it is possible that small amounts have remained in the final preparation. As the protein is in equilibrium with peptide-free buffer during the purification procedures, it is likely that those peptide-filled molecules that remain have high-affinity peptides bound to them that will not dissociate during the course of a binding experiment and therefore not interfere with the fast binding reaction.

Also, a partial dissociation of the complex of D^b heavy chain and hβ_2m into its components might complicate the kinetics of the heavy chain-peptide binding reaction (*14*). We have found no evidence that this process occurs under the conditions of our assays.

With the use of natural tryptophan fluorescence to monitor peptide binding to soluble purified class I heavy chain/β_2m complexes, we have taken care to choose a system that avoids all possible artifacts such as the modification of peptide, immobilization of the class I molecule, interference of other proteins, or presence of detergent. We believe that the fluorescence assay represents a true peptide binding event because the signal originates from the direct, and sequence-specific, interaction of the peptide with the protein. This is demonstrated by the fluorescence decrease upon addition of the GP-92-101 peptide and the lack of a change in the fluorescence signal when high concentrations of the irrelevant peptide, NP$_{68}$-91-99, are added (Figure 10). However, in the fluorescence assay, equilibrium association constant and dissociation rate are difficult to measure accurately: the former because of the low fluorescence signal at the D^b concentrations necessary to perform a titration experiment ($0.1-0.5 \times K_d$, or 2−10 nM) and the latter because of the insufficient baseline stability of fluorimetry equipment during the time required to measure dissociation of a high-affinity peptide from D^b ($\geq$ 20 h). Therefore, radioligand assays were still required to obtain accurate values for these constants. In control experiments, we have found that dissociation of the SV-324-332 peptide from D^b at 20 °C is undetectable in a 2.5 h fluorescence experiment (Figure 13) and that the affinity of the binding process measured by tryptophan fluorescence enhancement is $\geq 10^7$ M^{-1} (data not shown). Together with the demonstration of fast association rates in the radioligand assay (Figure 9) this provides strong evidence that both assays monitor the same direct and sequence-specific interaction of peptide and D^b/hβ_2m complex.

Fast Association Rates. We find that the specific binding of physiologically relevant peptides to D^b proceeds substantially faster in our system than previously reported for class I−peptide associations. This necessitated a stopped-flow approach to measure the association rate constants. The values that we have obtained, around 10^6 M^{-1} s^{-1} at 4 °C, are in accordance with association rates observed for peptides and small molecules binding to antibodies (*39*−*41*), enzymes (*42*), and cell surface receptors (*43*), which lie generally between 10^5 and 10^8 M^{-1} s^{-1}. The theoretical upper limit for a diffusion-controlled class I−peptide association reaction calculates as approximately 10^9 M^{-1} s^{-1} according to the Smoluchowski equation (*44*) (S. Springer, unpublished); the difference to our measurements is probably due to the fact that some spatial and conformational orientation of peptide and class I molecule has to take place before initial binding can occur.

The melting temperature (T_m) of the peptide binding site of the empty $D^b/h\beta_2m$ complex of 30.5 °C lies below the physiological temperature of 37 °C. Above the T_m, peptide binding slows down significantly to approximately 275 M^{-1} s^{-1} at 37 °C, or 6500-fold down from the rate observed at 16.5 °C. One possible explanation is that below the T_m, a highly peptide-receptive conformation of the D^b heavy chain is "frozen", which is only one of many possible structures of the molten binding site. To allow for fast peptide binding in vivo, this reversible denaturation of the binding site at 37 °C could be prevented by interaction with additional factors such as the peptide transporter TAP (*45*−*47*), the class I-binding protein Tapasin (*48, 49*) or the ER chaperones calnexin and calreticulin (*50*−*52*), all of which have been shown to interact with class I molecules at various stages of their biogenesis. They, or some as yet undescribed factor, could serve to hold the class I binding site in the peptide-receptive state.

Results from another recent study (*14*) suggest fast binding, on the order of 5×10^4 M^{-1} s^{-1} at 4 °C, of dansyl-labeled peptides to the H-2K^d class I molecule. Still, the association constants that we find using stopped-flow fluorescence spectroscopy at high ligand concentrations are about 30-fold higher (Table 1). Dissociation of dansylated peptides in that study proceeds biexponentially, with rates between 0.1 and 10^{-3} s^{-1} at 37 °C or between 6×10^{-4} and 2×10^{-5} s^{-1} at 4 °C. This is considerably faster than what we observe with unmodified peptides. Slower association, biexponential dissociation kinetics, and faster dissociation rates could all be due to the dansyl modification of the peptide side chains, which might lead to nonoptimal binding of the peptide; indeed, the authors observe that the place of attachment of the dansyl group to the peptide has a profound effect on equilibrium affinity and the kinetics of dissociation of the complex. Therefore, in that study, no mismatch of the kinetic to the equilibrium binding constants could be reported conclusively.

Mismatch of Kinetic and Equilibrium Constants. We have found the association rate constant for the SV-324-332 peptide at 4 °C to be 1500 times higher than predicted from the product of dissociation rate and equilibrium constant at this temperature. This leads us to propose that the binding of peptide to the D^b/β_2m dimer is not a simple one-step association/dissociation but governed by a more complex mechanism. Complicated ligand-binding kinetics frequently indicate the conformational isomerization of a receptor (*29*) or antibody (*39, 53*) in the binding process. Viewed from a different perspective, the equilibrium affinity constant that we observe, and therefore the binding energy of the class I−peptide complex, is 1500 times lower than predicted from the ratio of the kinetic constants, suggesting that part of the binding energy is used by the protein to undergo a conformational change, thereby leading to a lower apparent equilibrium association constant (*54, 55*).

A conformational change of the class I molecule upon peptide binding has indeed been proposed from the study of the crystal structures of HLA-A2 (*56*), H-2K^b (*57*), H-2D^b (*35*), and other class I molecules (*58*). In these crystals, a large proportion of the peptide surface is buried in the class I binding groove (*59*). The crystal structure of the complex of NP_{68}-366-374 with H-2D^b shows that 76.4% of the surface of this peptide is buried in the bound state. It has been assumed that these complexes could not form without a conformational rearrangement of the binding site during peptide binding. Our observations now provide experimental evidence in support of this hypothesis.

Upon the addition of peptide (*60*) or β_2m (*8*), free D^b heavy chains in detergent acquire the epitope for the monoclonal antibody B22.249 (*31*). The acquisition of this epitope is not identical to the conformational change of the D^b binding site that we propose but lies earlier on the complex formation pathway. The empty soluble D^b molecules described in this study have β_2m bound to them when they are isolated and can therefore be precipitated with B22.249 before they are exposed to peptide (Figure 3).

In MHC class II molecules, a conformational change upon peptide binding has been demonstrated by SDS gel mobility analysis (*61, 62*). The authors suggest that the peptide first binds to the class II molecule to form an intermediate that slowly rearranges to the stable complex, a common mechanism in receptors (*42*). We have been unable to detect any signs of an unstable, fast-dissociating intermediate in the peptide-D^b binding process that should be present in considerable amounts at early time-points of the reaction; in contrast, the fast binding reaction already appears to be essentially irreversible (Figure 13). Additionally, when compared to MHC class II molecules and other proteins that undergo conformational changes upon ligand binding (*42, 43, 63*), the mismatch between predicted and found association rate, 3 orders of magnitude, seems exceptionally large in H-2D^b. For these two reasons, we think that the first, fast-binding step, as monitored by tryptophan fluorescence, might be followed by several rearrangement steps that could be essentially irreversible. These might represent the folding of the hydrophobic binding site around the peptide, giving rise to its buried appearance in the crystal structure. In another hypothetical scheme, a rapidly formed kinetic intermediate could proceed both in a productive manner, giving rise to a stable complex, and nonproductively, leading to its dissociation.

This proposal of a conformational change in the binding site of the D^b/β_2m complex upon peptide binding implies that when class I molecules first interact with peptide, they may be in a conformation that is different from the equilibrium structure observed in crystallographic studies. This "encounter complex" formed on first contact with the peptide could comprise fewer, or different, interactions of the class I heavy chain with the peptide. Additional evidence for this hypothesis comes from our observation that the association rate constant is only weakly influenced by variations of the peptide sequence: if glycine is substituted for the anchor residue methionine in position 9 of the NP_{68}-Y367-374 peptide, the association rate constant only decreases by 2.8-fold (Table 1). Likewise, if the peptide's C-terminus is extended by five amino acids, the decrease in the association rate is only 5.6-fold. Although we have not obtained equilibrium affinity data for these peptides due to the difficulty of labeling methionine-containing peptides with tritium, earlier data using iodinated peptides in detergent cell lysates suggest that for the elongated peptide the equilibrium constant may decrease by as much as factor 40 (*3*). This provides a second line of evidence that initial binding of peptides to D^b/β_2m occurs with relaxed specificity compared to equilibrium binding requirements.

In the same study, it was demonstrated that complexes of D^b/β_2m with altered or elongated peptides have substantially shorter half-lives (i.e., substantially higher dissociation rate constants) than those with optimal peptides. They are, therefore, more likely to dissociate while still in the ER or before reaching the cell surface. These peptides with higher dissociation rates are also far less effective than the optimum-length peptide in sensitizing target cells for CTL lysis. Recently, other studies have confirmed this connection between the dissociation rate constant from class I molecules and the in vivo immunogenicity of epitope peptides (*64*, *65*).

These observations support the hypothesis that in vivo, fast on-rates, combined with relaxed initial specificity, allow class I molecules to bind a wide range of peptides into an "encounter complex". Only a subset of these encounter complexes then becomes permanent and accumulates at the cell surface. In this model, peptide selection by class I molecules would occur in two stages: first, at the initial binding reaction, and second, when dissociation of low-affinity peptides from initially formed encounter complexes takes place. Selection of peptides at either stage is likely to be governed by a sum of peptide−class I interactions that is different from what is seen in crystallographic structures. To fully understand the rules of MHC class I−peptide selection, these interactions must therefore be taken into account. Further kinetic investigation of both stages of peptide binding will then extend the understanding of class I−peptide binding specificity and peptide selection beyond the limits of equilibrium measurements.

ACKNOWLEDGMENT

We thank Drs. Don Mason for discussions, Sheena Radford and Michael Gross for the use of the stopped-flow equipment, Dennis Benjamin for mass spectroscopy data, Jörn Werner for help with the preparative ultracentrifugation, and Diana Cowley and Jonathan Edwards for excellent technical support. S.S. wishes to express his gratitude to Prof. Randy Schekman. S.S. was supported by a Wellcome Trust Prize Studentship and by the Townsend-Jeantet Prize Trust. V.C. is a Senior Fellow of the Medical Research Council of Great Britain.

REFERENCES

1. Neefjes, J., Momburg, F., and Hämmerling, G. (1993) *Science 261*, 769−771.
2. Townsend, A., Rothbard, J., Gotch, F., Bahadur, B., Wraith, D., and McMichael, A. (1986) *Cell 44*, 959−968.
3. Cerundolo, V., Elliott, T., Elvin, J., Bastin, J., Rammensee, H.-G., and Townsend, A. (1991) *Eur. J. Immunol. 21*, 2069−2075.
4. Falk, K., Rötzschke, O., Stevanovic, S., Jung, G., and Rammensee, H.-G. (1991) *Nature 351*, 290−296.
5. Madden, D., Gorga, J., Strominger, J., and Wiley: D. (1991) *Nature 353*, 321−325.
6. Elliott, T., Elvin, J., Cerundolo, V., Allen, H., and Townsend, A. (1992) *Eur. J. Immunol. 22*, 2085−2091.
7. Matsumura, M., Saito, Y., Jackson, M., Song, E., and Peterson, P. (1992) *J. Biol. Chem. 267*, 23589−23595.
8. Townsend, A., Elliott, T., Cerundolo, V., Foster, L., Barber, B., and Tse, A. (1990) *Cell 62*, 285−95.
9. Elliott, T., Cerundolo, V., Elvin, J., and Townsend, A. (1991) *Nature 351*, 402−6.
10. Neefjes, J., Hämmerling, G., and Momburg, F. (1993) *J. Exp. Med. 178*, 1971−1980.
11. Burshtyn, D. N., and Barber, B. H. (1993) *J. Immunol. 151*, 3082−93.
12. Margulies, D. H., Corr, M., Boyd, L. F., and Khilko, S. N. (1993) *J. Mol. Recognit. 6*, 59−69.
13. Fahnestock, M. L., Johnson, J. L., Feldman, R. M., Tsomides, T. J., Mayer, J., Narhi, L. O., and Bjorkman, P. J. (1994) *Biochemistry 33*, 8149−58.
14. Gakamsky, D. M., Bjorkman, P. J., and Pecht, I. (1996) *Biochemistry 35*, 14841−14848.
15. Boyd, L. F., Kozlowski, S., and Margulies, D. H. (1992) *Proc. Natl. Acad. Sci. U.S.A. 89*, 2242−6.
16. Olsen, A. C., Pedersen, L. O., Hansen, A. S., Nissen, M. H., Olsen, M., Hansen, P. R., Holm, A., and Buus, S. (1994) *Eur. J. Immunol. 24*, 385−392.
17. Ojcius, D. M., Abastado, J. P., Casrouge, A., Mottez, E., Cabanie, L., and Kourilsky, P. (1993) *J. Immunol. 151*, 6020−6.
18. Ojcius, D. M., Godeau, F., Abastado, J. P., Casanova, J. L., and Kourilsky, P. (1993) *Eur. J. Immunol. 23*, 1118−24.
19. Cerundolo, V., Elliott, T., and Townsend, A. (1992) *Prog. Immunol. VIII*, 175−180.
20. Chen, W., Khilko, S., Fecondo, J., Margulies, D. H., and McCluskey, J. (1994) *J. Exp. Med. 180*, 1471−83.
21. Khilko, S. N., Jelonek, M. T., Corr, M., Boyd, L. F., Bothwell, A. L., and Margulies, D. H. (1995) *J. Immunol. Methods 183*, 77−94.
22. Neefjes, J. J., Dierx, J., and Ploegh, H. L. (1993) *Eur. J. Immunol. 23*, 840−5.
23. Dornmair, K., Clark, B. R., and McConnell, H. M. (1991) *Proc. Natl. Acad. Sci. U.S.A. 88*, 1335−8.
24. Tussey, L. G., and Frelinger, J. A. (1991) *Hum. Immunol. 32*, 183−93.
25. Buelow, R., Kuo, S., Paborsky, L., Wilson, K. J., and Rothbard, J. B. (1994) *Eur. J. Immunol. 24*, 2181−5.
26. Bebbington, C. R. (1991) *Methods 2*, 136−145.
27. Allen, H., Wraith, D., Pala, P., Askonas, B. A., and Flavell, R. A. (1984) *Nature 309*, 279−282.
28. Fahnestock, M. L., Tamir, I., Narhi, L., and Bjorkman, P. J. (1992) *Science 258*, 1658−1662.
29. Hulme, E. C., and Birdsall, N. J. M. (1992) in *Receptor−Ligand Interactions: A Practical Approach* (Hulme, E. C., Ed.) pp 63−176, Oxford University Press: Oxford.
30. Crowe, J., Dobeli, H., Gentz, R., Hochuli, E., Stuber, D., and Henco, K. (1994) *Methods Mol. Biol. 31*, 371−87.
31. Hämmerling, G. J., Hämmerling, U., and Lemke, H. (1979) *Immunogenetics 8*, 433−445.
32. Gill, S. C., and von Hippel, P. H. (1989) *Anal. Biochem. 182*, 319−326.
33. Schumacher, T. N., De, B. M., Vernie, L. N., Kast, W. M., Melief, C. J., Neefjes, J. J., and Ploegh, H. L. (1991) *Nature 350*, 703−6.
34. Lehrer, S. S., and Fasman, G. D. (1967) *J. Biol. Chem. 242*, 4644−4651.
35. Young, A. C. M., Zhang, W., Sacchettini, J. C., and Nathenson, S. G. (1994) *Cell 76*, 39−50.
36. Gairin, J. E., Mazarguil, H., Hudrisier, D., and Oldstone, M. B. (1995) *J. Virol. 69*, 2297−2305.
37. Van Gilst, M., Tang, C., Roth, A., and Hudson, B. (1994) *J. Fluor. 4*, 203−208.
38. Roughton, F. J. W., and Chance, B. (1963) in *Techniques of organic chemistry* (Freiss, S. L., Lewis, E. S., and Weissberger, A., Eds.) pp 703−798, Wiley-Interscience, New York.
39. Pecht, I. (1983) in *Protein conformation as an immunological signal* (Celada, F., Schumaker, V. N., and Sercarz, E. E., Eds.) pp 3−13, Plenum Press: New York.
40. Foote, J., and Milstein, C. (1991) *Nature 352*, 530−532.
41. Zeder-Lutz, G., Altschuh, D., Geysen, H. M., Trifilieff, E., Sommermeyer, G., and Van Regenmortel, M. H. (1993) *Mol. Immunol. 30*, 145−55.
42. Gutfreund, H. (1995) *Kinetics for the life sciences*, Cambridge University Press, Cambridge (U.K.).
43. Fersht, A. (1984) *Enzyme structure and mechanism*, W. H. Freeman and Company, New York.
44. von Smoluchowski, M. (1917) *Z. Phys. Chem. 92*, 129−168.

45. Suh, W., Cohen, D., Fruh, K., Wang, K., Peterson, P., and Williams, D. (1994) *Science 264*, 1322−1326.
46. Ortmann, B., Androlewicz, M. J., and Cresswell, P. (1994) *Nature 368*, 864−7.
47. Neisig, A., Wubbolts, R., Zang, X., Melief, C., and Neefjes, J. (1996) *J. Immunol. 156*, 3196−206.
48. Sadasivan, B., Lehner, P. J., Ortmann, B., Spies, T., and Cresswell, P. (1996) *Immunity 5*, 103−14.
49. Ortmann, B. et al. (1997) *Science 277*, 1306−9.
50. Degen, E., Cohen-Doyle, M., and Williams, D. (1992) *J. Exp. Med. 175*, 1653−1661.
51. Sugita, M., and Brenner, M. B. (1994) *J. Exp. Med. 180*, 2163−2171.
52. Solheim, J. C., Carreno, B. M., and Hansen, T. H. (1997) *J. Immunol. 158*, 541−3.
53. Foote, J., and Milstein, C. (1994) *Proc. Natl. Acad. Sci. U.S.A. 91*, 10370−10374.
54. Chothia, C., and Janin, J. (1975) *Nature 256*, 705−708.
55. Franklin, T. J. (1980) *Biochem. Pharmacol. 29*, 853−856.
56. Madden, D. R., Gorga, J. C., Strominger, J. L., and Wiley, D. C. (1993) *Cell 75*, 693−708.
57. Fremont, D. H., Matsumura, M., Stura, E. A., Peterson, P. A., and Wilson, I. A. (1992) *Science 257*, 919−927.
58. Madden, D. R. (1995) *Annu. Rev. Immunol. 13*, 587−622.
59. Stanfield, R. L., and Wilson, I. A. (1995) *Curr. Opin. Struct. Biol. 5*, 103−113.
60. Elliott, T., Cerundolo, V., Townsend, A. (1992) *Eur. J. Immunol. 22*, 3121−3125.
61. Dornmair, K., Rothenhausler, B., and McConnell, H. M. (1989) *Cold Spring Harbor Symp. Quant. Biol. 44*, 409−416.
62. Sadegh-Nasseri, S., and Germain, R. (1991) *Nature 353*, 167−169.
63. Strickland, S., Palmer, G., and Massey, V. (1975) *J. Biol. Chem. 250*, 4048−4052.
64. van der Burg, S. H., Visseren, M. J., Brandt, R. M., Kast, W. M., and Melief, C. J. (1996) *J. Immunol. 156*, 3308−14.
65. Sijts, A. J., and Pamer, E. G. (1997) *J. Exp. Med. 185*, 1403−11.

BI9717441